Computational Flow Field Analysis around a Single Wrap-around Fin

Nayhel SHARMA*,[1], Gurteg Singh NAGI[1], Hrishabh CHAUDHARY[1], Palak SAINI[1], Rakesh KUMAR[1]

*Corresponding author
[1]Aerospace Engineering Department,
Punjab Engineering College (Deemed to be University),
Chandigarh, India,
nayhelsharma@gmail.com

DOI: 10.13111/2066-8201.2020.12.2.17

Received: 29 January 2020/ Accepted: 10 April 2020/ Published: June 2020

Abstract: *A flow field aerodynamic analysis using Computational Fluid Dynamics (CFD) model of a single wrap around fin is performed at 0° angle of attack and its flow visualizations are presented in this paper for a subsonic to supersonic Mach range. A comparative study is performed by utilizing two WAF geometries aligned in opposite directions and with different edges (Sharpened and Blunt). The aerodynamic characterization has been conducted using a realizable κ-ϵ turbulence model utilizing a high-quality mesh to understand the nuances of the flow around the curved fin structure. The quantities of interest are the computed aerodynamic coefficients which have been validated with their precursors. By investigating the contours of the pressure coefficient and the relative Mach number, the flow phenomenon in the vicinity of the curved fin can be understood in a finer way.*

Key Words: *CFD, Aerodynamics, Wrap-around fin*

1. INTRODUCTION

Background. The Wrap-around fins (WAFs) have been in use for tube launched projectiles due to their body enveloping ability. The WAFs stowing capabilities and versatility have attracted many investigators in the past. However, the instabilities which are inherent to WAFs due to their asymmetric geometry (curved surface) especially in the transonic regime have always been a key area of interest for the researchers. The aerodynamics of flow around the fin as well as the fin passage (area between the two adjoining fins) have been examined time and again for their aerodynamic improvement. It has been illustrated that at 0° angle of attack the pressure on both sides of the fins is different [1]. The flow around the fins is influenced by the fin leading as well as its trailing edge, hence many studies have been carried out on reducing the fin anomalies by changing the leading edge of the fin. The Roll reversal that is observed in the transition from subsonic to supersonic speeds at 0° angle of attack is a major setback for these fins, in addition to the display of pitch-yaw coupling [2]–[5]. A key aspect in these findings is the observance of shock structures near these fins which are deemed to be the reason for the loss of static stability of such projectiles [4]. The pressure differences on the concave and the convex side of the fins seemed to incubate the rolling moment. The previous studies show the existence of vortex at the root of the fin i.e. the fin-missile body juncture.

Computational Studies. The CFD on the missiles with wrap-around configurations [1], [6]–[13] showed general agreement with the experimental studies [4], [14]–[19]. Bagheri [1], et al. conducted an inviscid CFD study comparing the drag and lateral moment coefficients of conventional WAFs with opposite oriented WAFs, and finding the later more useful. Li [6], et al. estimated the aerodynamic characteristics of a missile with wrap-around fins using a $\kappa - \omega$ transition shear stress transport (SST) turbulence model in the Mach number range of 1.6 to 5. Liu [7], et al. compared the wrap-around fins with the planar fin missile model computing the lift, drag, roll coefficients of the missile in the Mach number range 0.6M to 3.0M. Their computations were based on one equation Spalart-Allmaras turbulent model and the main difference was found in the rolling moment coefficients.

Krishna [8], et al computed the flow field solutions of missiles with WAFs focusing on the leading edge of the fins and their fin passage in the Mach number range of 1.2 to 2.5. Mao [9], et al. conveyed the effects of setting an angle of WAFs on rolling and pitching moment of the missile. Rolling Moments were computed by S. Mandić [10] between angle 0°and 0.8°, similar work on computation of rolling moments using CFD was done by Paek [11], et al. using the Euler equations.

Edge [12] successfully calculated the aerodynamic coefficients of the missile with WAFs using CFD in the Mach number range of 1.3 to 3.0.

Single Fin Model. Tilman [20]–[24], et al. both experimentally and computationally investigated a single wrap-around fin model at freestream Mach numbers [~2.8,2.9]. The characterization of flow around a single fin was performed numerically at freestream Mach numbers [~2.8,2.9M] [22], [23].

These numerical studies were based upon the Baldwin and Lomax model of turbulence [25]. The predicted results of the inviscid simulations, especially the rolling moment coefficients [22] when multiplied by four, seemed to agree with the earlier inviscid calculations [26] which motivated to extend this research using recent computational methods. Sharma [27]–[30], et al. reviewed various CFD studies on WAFs [27] and performed a visual comparative validation study of a single fin WAF [28].

A study was carried out using a single generic planar fin configuration [29], and finally a comparison was carried out between a single planar fin and WAF [30]. In the study [30], the aerodynamics of a single planar fin having blunt leading edge were compared with a single WAF having sharpened edges.

Also, the validation of a single fin missile model with a full four fin missile model was established. This study mainly dealt with static pressure and Mach number contours around the sharpened edged WAF model, which may be of limited value to the readers, therefore setting up a need for transparent communication.

The geometric influence on the aerodynamics of WAF has been presented in the current study by comparing an oppositely aligned, blunt edged WAF with a sharpened edged WAF. Hence, in the current study, contours of pressure coefficients and free stream velocities (non-dimensional results) were chosen to be presented along with comprehensive solver selection criteria.

The current study compliment and expands on the lack of an insight to the solver selection (validation) and the computational setup. The major objectives of this paper were to:

(1) Compare and understand the aerodynamics and flow behaviour on adapting a single blunt edged WAF, aligned inversely in the flow direction;

(2) Present a comprehensive solver validation of a single fin missile model;

(3) Present an exhaustive flow field visualisation of pressure coefficients and relative Mach number contours (Non-Dimensional) along with their Cumulative aerodynamic coefficients.

2. NUMERICAL METHODOLOGY

Geometry. A complete missile body with an ogive nose was cut in such a way that it formed a semi-cylinder like body, with a fin mounted at the tail end of the model and same as that of Sharma [27], [30] et al. The dimensions of this model were such that it represented a complete Missile body of that of Vitale [4] et al. The true length of the model is 0.147*m* with maximum height of the semi-cylinder at 0.00795*m*, with *AR*= ~1 of the fin. The thickness of the fin was kept at 0.00254*m.* Additional set of computations were performed involving an identical oppositely aligned blunt edged single fin WAF geometry model with *AR*= ~1. The dimensions of the semi-cylindrical model remained the same as that of the above-mentioned geometry however for the better understanding of the new model geometry changes are presented in *Figure 1(a-c).*

Meshing Details. A completely structured Mesh involving multiple o-grids (*an ICEM® Feature*) consisting of Hexa-dominant elements was employed in the computations [30]. The mesh sensitivity was confirmed by comparing the drag coefficient values for four different mesh sizes at Mach 2.8.

These mesh sizes varied from 1.33 million cells to 1.92 million cells. The minimum computed value of drag coefficient was 0.379623 for the mesh with 1.33 million cells and the maximum value obtained was 0.38762103 for the mesh with 1.47 million cells.

Therefore, a mesh with 1.45 million cells was adopted for all the computations consisting of sharpened edged WAF.

In the case of a blunt edged WAF a mesh with 0.7 million cells was considered, this mesh had a remarkable Minimum Orthogonal Quality = 6.34240e-01, therefore a grid sensitivity test did not seem to be necessary in this case.

Flow and Solver Details. The computational domain remained similar for both the models, which consisted of an inlet quarter sphere, the far-field and the outlet surface, which have already been defined earlier and the details of their flow parameters and the solver are in the scope of *reference* [30].

The Solution methods were based on choosing the most attractive parameters mentioned in the review of previous computational studies on WAFs [27]. The summary of the flow conditions as well as the solver adaptions have been mentioned in *Tables 1* and *2*. The fundamental governing equations remain the continuity equation, the momentum equation and the energy equation [27], [30], [31] and the turbulence closure was carried out with two equation Realizable - $\kappa - \epsilon$ turbulence model [32]. The term "realizable" means that the model satisfies certain mathematical constraints on the Reynolds stresses, consistent with the physics of turbulent flows [33]. An additional solution method approach was endorsed using Roe-FDS scheme for subsonic Mach number simulations.

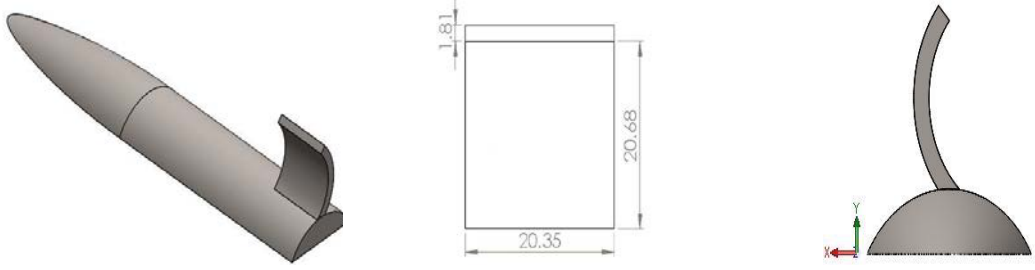

(a) (b) (c)

Figure 1: (a) Blunt Edged Single WAF model; (b) Span and Chord of the Blunt edged fin (in mm); (c) Front view of the Blunt Fin WAF Model

Table 1: Summary of the flow conditions applied in the numerical simulations that were carried out

Freestream Velocity Corresponding to Mach Number (m/s)	**Air Density**	**Temperature (Kelvin)**	**Pressure (Pascal)**	**Boundary Conditions at the Inlet, Outlet & Far-field**	**Missile and Fin Body**
136.03 - 1020.225 m/s	*Ideal Gas – 1.22 kg/m³*	*288K*	*101325Pa*	*Pressure far-field conditions*	*No-slip wall Condition*

Table 2: Solver Details

Solver Type	**Solution Method**	**Spatial Discretization**
Time Steady Density Based	*Implicit Formulation with flux type - Advection Upstream Splitting Method (AUSM) and Roe-FDS in some planar subsonic computations*	*Least Square Cell Based Second Order Upwind*

Solver Validation Study: Iterative convergence of the Normalized Residuals. A strict convergence criterion was set up for each computation, the initial solution guess was predicted utilizing the first order upwind discretization (flow Variables) in which all the residuals were brought below the order of 1E-5.

In the case of sharpened WAF case the initial solution took around 8000 to 1200 iterations to converge.

Subsequently, a second order discretization (for all variables) was applied to the initial guess in which all the residuals were brought down to the order of 1E-4; this took additional 400 to 600 iterations.

The convergence of the normalized residuals in the case of Blunt edged WAF took lesser number of iterations.

On utilizing the first order upwind discretization (flow variables) all the residuals were brought to the order of 1E-5; this took around 250 to 1000 iterations and subsequently on applying the second order of discretization, all the residuals were brought down to the order of 1E-4, this took around 200 to 600 additional iterations.

Residual convergence history of the sharpened and blunt edged Single WAF, respectively, have been reported in *Figure 2(a-d)* for both subsonic and supersonic Mach regimes. It must be mentioned here that Courant-Friedrichs-Lewy (CFL) number was ramping up was done in almost all the computations resulting in a speedier convergence process.

After gaining confidence in the residual convergence, in some cases (mostly supersonic) the second order of discretization was directly applied for convergence and the residuals were brought down to the order of 1E-4, in around 250 iterations *Figure 2(d)*.

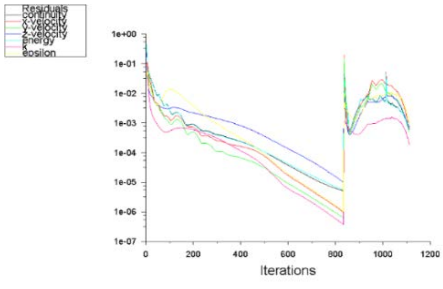

(a)

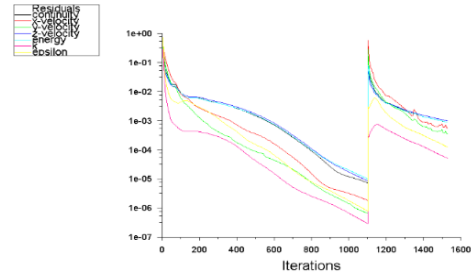

(b)

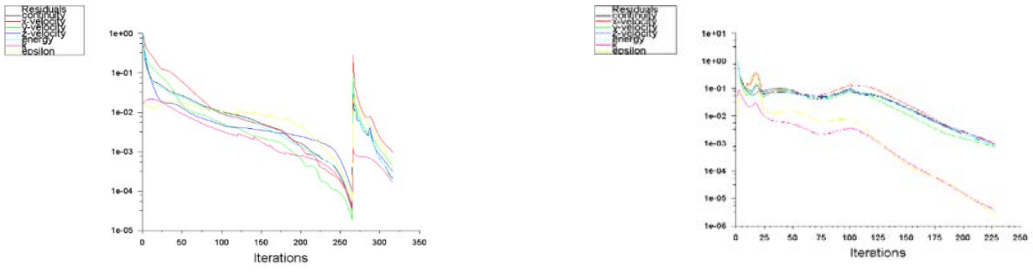

(c) (d)

Figure 2: Residual Convergence of Sharpened Edged Single WAF at (a) Subsonic Mach Number (~0.6M); (b) Supersonic Mach Number (~2.6); (c) Blunt Edged Single WAF at Mach 0.8; (d) Blunt Edged Single WAF at Mach 2.6

Selection of Turbulence Model and Validation of Computed Results. For the purpose of selection of turbulence closure model, a comparison study was carried out between the computed results of one equation Spalart-Allmaras *(S-A)* and the two-equation realizable $\kappa - \epsilon$. It was done by computing, comparing and analysing the obtained drag and moment coefficients (Sharpened edged WAF) with both experimental and computational results available from the prior studies *(Figures 3-6)*.

The computed drag coefficients using the *(S-A)* and the two-equation realizable $\kappa - \epsilon$ models nearly overlapped each at some instances, however the results from the later were virtually indistinguishable when compared to the experimental results at Mach 1, 1.2, 1.8, and 3. The obtained drag coefficients were compared with the prior computational results, and the realizable $\kappa -$, result in lesser error margin as compared to the *S-A* model.

In order to reaffirm the confidence in the selection of turbulence model, the computed moment coefficients were also compared with the prior experimental and computational results.

The change in the sign of rolling moment was more accurately captured at Mach ~1.2 using the two-equation realizable $\kappa - \epsilon$ model and at a much later Mach (~1.5) while using the *S-A* model of turbulence.

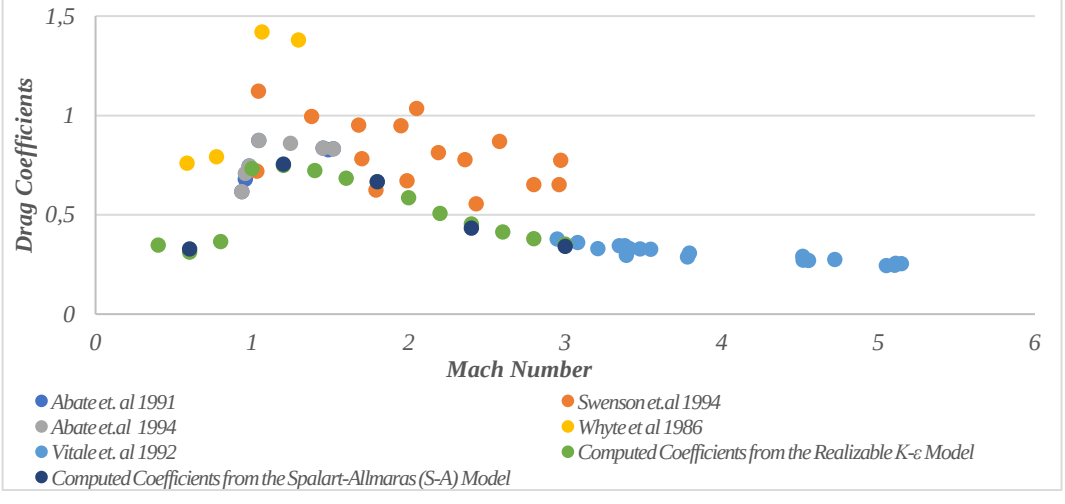

Figure 3: Comparison of the evaluated Drag Coefficients values at different Mach numbers from the two different turbulence models (i.e. K-ε and S-A) with the results from prior experimental studies

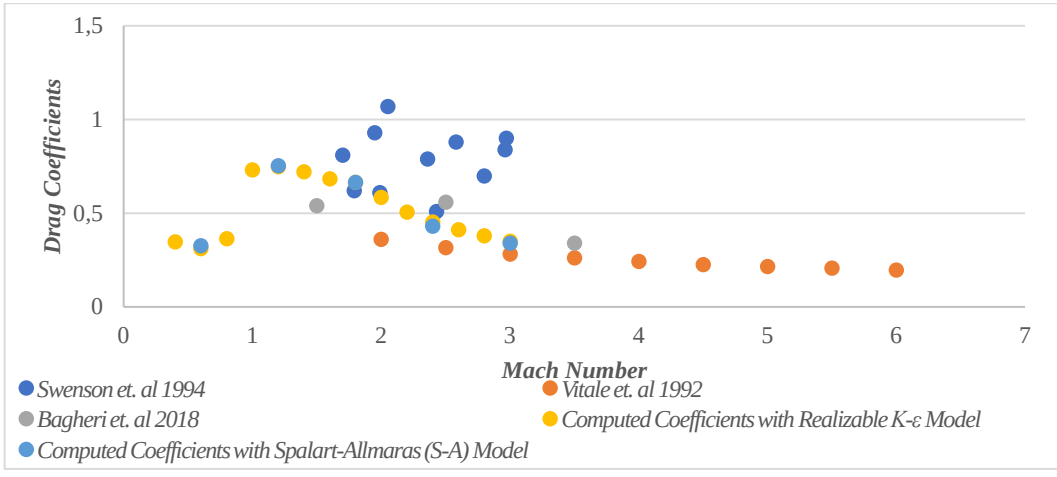

Figure 4: Comparison of the evaluated Drag Coefficients values at different Mach numbers from the two different turbulence models (i.e. K-ε and S-A) with the results from prior computational studies

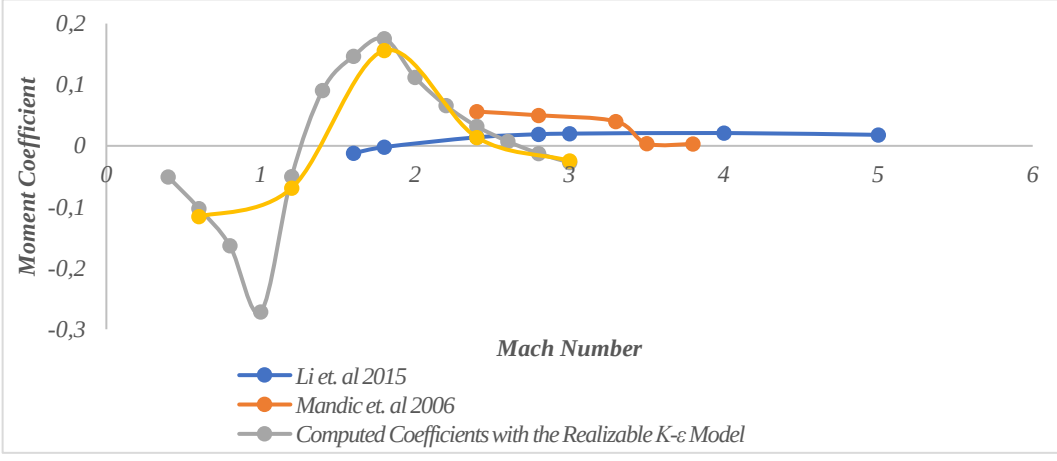

Figure 5: Comparison of the evaluated Moment Coefficients values at different Mach numbers from the two different Turbulence models (i.e. K-ε and S-A) with the results from the prior experimental studies.

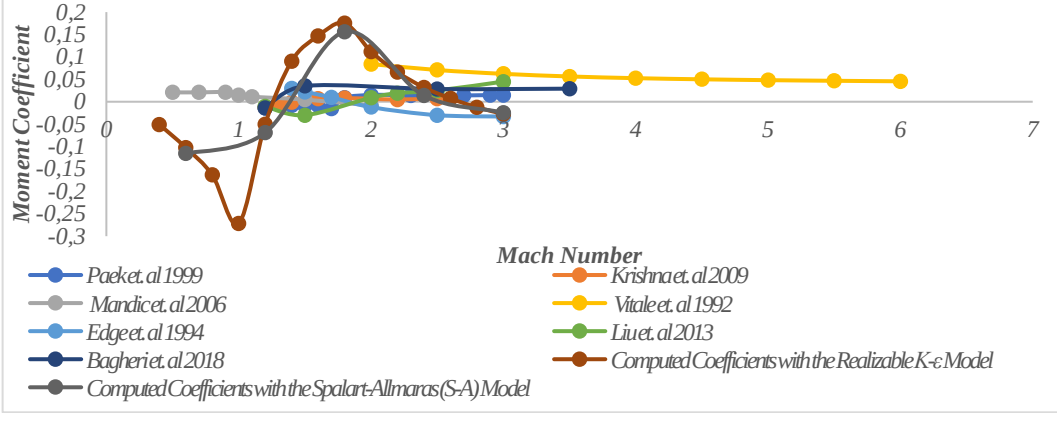

Figure 6: Comparison of the evaluated Moment Coefficients values at different Mach numbers from the two different Turbulence models (i.e. K-ε and S-A) with the results from the prior computational studies.

3. RESULTS

The Force and the Moment Coefficients. The comparison of the force (Drag) coefficients and the moment coefficients of both Sharpened edges and the blunt edged WAFs have been presented in this section.

The drag Coefficients of the complete missile models were calculated by choosing the reference area $A_{Ref} = \pi R^2$, and reference length $L_{Ref} = R$, where *R= 7.95mm.*

The basis of selection of this area and length values were based on previous studies [6], [11], [13], [30].

The fin drag coefficient (Fin alone) along with the drag coefficients of the full single fin models, have also been compared and their values have been presented in *Figure 7.* The missile model with blunt WAF showed increment in the drag coefficient values when compared to the sharpened edged single fin WAF.

The overall drag coefficient values of the blunt edged WAF model were 9.0781% to 62.49324% greater as compared to the Sharpened edged WAF with the smallest difference in the value at Mach 1.4 and maximum at Mach 3.0. It is interesting to note that the Fin alone contribution towards the overall Drag Coefficients of the model was 18.7522% to 53.1864% in the case of blunt fin WAF.

The maximum contribution of the fin alone drag was at Mach 1.0 and the least at Mach 3.0 in the case of Blunt WAF.

On the contrast the fin alone drag contribution in the case of sharpened edged WAF varied from 37.9788% to 44.7710%, with the least value at Mach 0.8 and maximum at Mach 3.0.

The average contribution of the Fin alone drag coefficient was 29.9600% in the case of blunt edged WAF and 42.1846% in the case of the sharpened Fin alone WAF.

The sharpened edged single fin missile model indicated 37.4115% reduction the overall drag values.

The computed roll moment coefficient values have been presented in *Figure 8.* Prior to comparing and analysing the moment coefficient values, it should be made clear that the "Direction Changed" mentioned with blunt edged WAF means that the moment coefficients were multiplied with "-1" before plotting.

This was done to compliment the effect of opposite alignment of the blunt WAF in the result values.

On examining the roll moment coefficients, it can be observed that the sharpened edged WAF model exhibits change in moment direction at ~1.2M whereas in the case of Blunt edged WAF the moment coefficients change their sign ~1.6.

These results are of significance as Mach 1.2 is the nearly the same Mach number at which the roll moment coefficient changed sign in the previous experimental studies [27], [30].

Also, for the case of blunt edged WAF, the critical Mach number (Mach at which the roll moment coefficients changed their sign/direction) is stated much later ~1.6M for a blunt shaped WAF [12].

At supersonic Mach numbers especially above Mach 1.2, the blunt WAF indicate stronger moment coefficient forces as compared to the sharpened edged WAF.

The moment forces at these Mach numbers (greater than Mach 1.2) produced by the blunt edged WAF were on an average 66.97% stronger than the forces produced by the sharpened edged WAF.

The sharpened edged WAF showed second roll reversal above ~2.2M however there were no indications in the roll reversal of blunt edged WAF up to Mach 3.0.

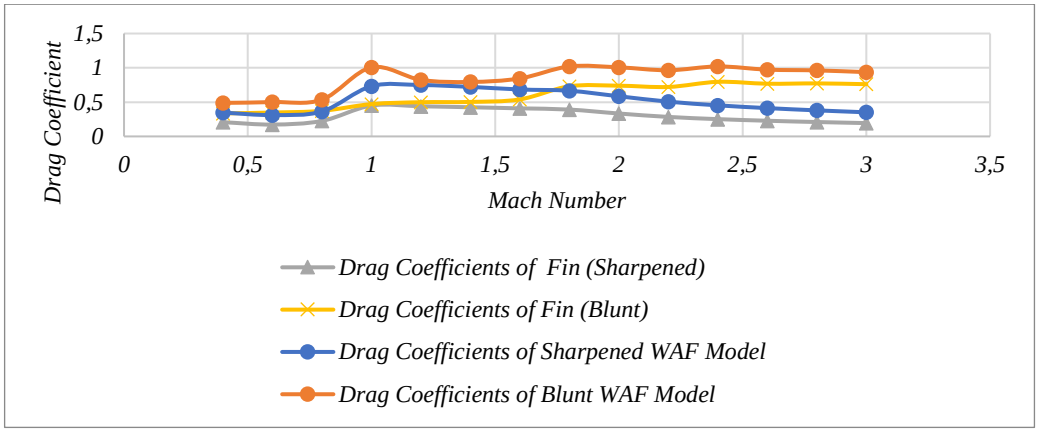

Figure 7: Comparison of Drag Coefficients of Sharpened and Blunt Fin WAF model

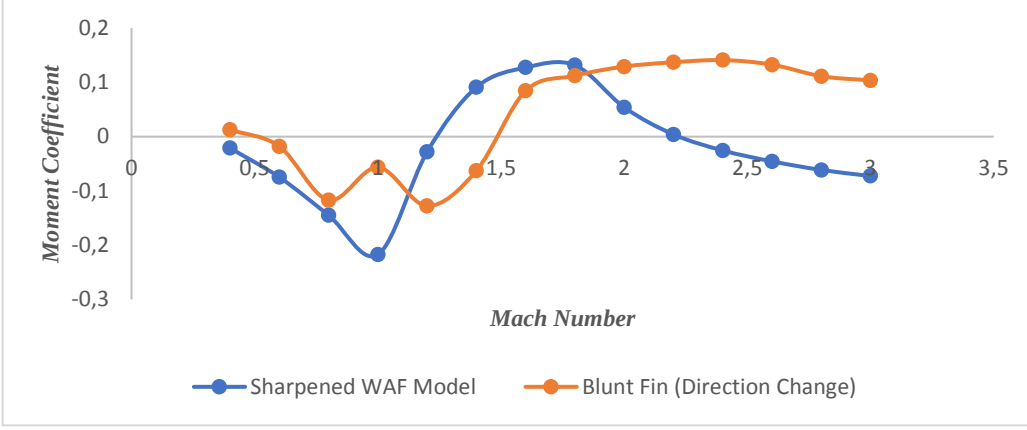

Figure 8: Comparison of Moment Coefficients of Sharpened and Blunt Fin WAF model

Flow visualizations: The flow visualizations obtained from the current computations of both Sharpened edged and the oppositely aligned blunt edged WAF are presented in this section. It can be observed from *Figures 7* and *8*, that the prominent Mach numbers for the both types of WAF configurations influencing the flow physics are in the range between Mach 0.8 to 1.8. Therefore, the non-dimensional pressure and the Mach number contours have been presented in this section for better perception of the flow phenomenon in the above-mentioned governing Mach range. Both the sharpened edged and the blunt edged WAF models have been considered simultaneously for better comparison at similar Mach numbers. The flow visualizations consist of five sections, out of which the first four sections are dedicate to the pressure coefficient contours. These pressure contours are presented as *(i)* Surface pressures on the missile model, *(ii)* Flow pattern at the mid-plane around the model, *(iii)* Pressure coefficient contours around the fins, starting from the root of the fin, till the top of the fin, *(iv)* Relative Mach number contours on the model surfaces (visualizations presented for both sharpened and the blunt edged fins), *(v)* Pressure coefficient contours along the fins in the longitudinal direction starting from the fin tip leading edge till the trailing edge of the fin. The first set of images consists of pressure coefficient contours on the surfaces of the WAF models, at Mach 0.8-1.8. These surface contours images consist of top view (on the left part of the image) and the side views (both convex and the concave side of the fins). *(Figures 9-14)* At Mach 0.8 both the sharpened and the blunt edged WAF exhibit higher pressures on the convex

side of the fin, however these forces commence on the sharpened edged WAF prior to the blunt edged WAF. There is a considerable contrast in the pressure coefficients of both the models at Mach 1.0, the sharpened edged WAF depict high pressure rise ahead of the convex side, and a sudden pressure drop in the case of blunt edged WAF, though the pressures on the convex side in the blunt edged fin remain higher as compared to the blunt edged. At Mach 1.2 the surface pressures on both sides of the fins shift towards identical patterns, depicting equivalence of pressures on both sides of the sharpened edged fins. A significant pressure drop can be observed on the concave side of the blunt edged WAF at Mach 1.2. Identical pressure contours on the concave and convex surface of the sharpened WAF, initiate to disparate at Mach 1.4 however, the pressure contours incept to complement each other at Mach 1.4 in the case of blunt edged WAF. At Mach 1.6 the high-pressure contours ahead of the leading edge of the sharpened fins become observable, reaffirming the change in the roll direction. It is at Mach ~1.6 where indistinguishable pressure contours appear on the concave and the convex side of the blunt edged WAF. Therefore, reaffirming the delayed critical Mach number at which the roll reversal takes place. High pressure region emancipates ahead of the blunt leading edge of the fin endorsing the roll reversal at Mach ~1.8. On considering the pressure contours on the either sides of the sharpened edged WAF inception of its second phase of roll reversal at Mach 1.8 is perceivable.

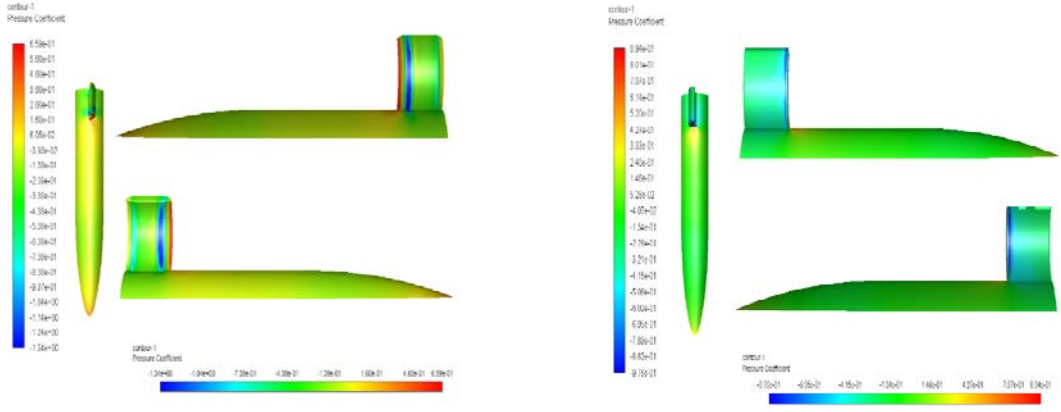

(a) (b)

Figure 9: (a) Sharpened Edged, (b) Blunt edged; Mach 0.8

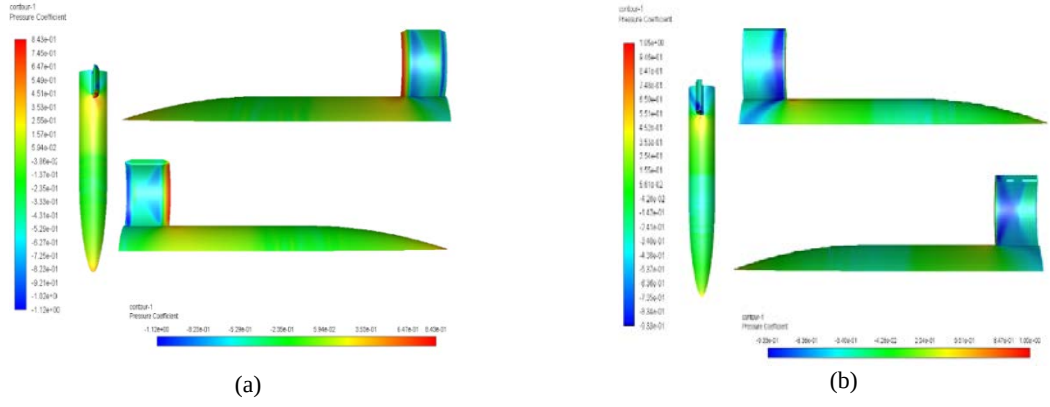

(a) (b)

Figure 10: (a) Sharpened Edged, (b) Blunt edged; Mach 1.0

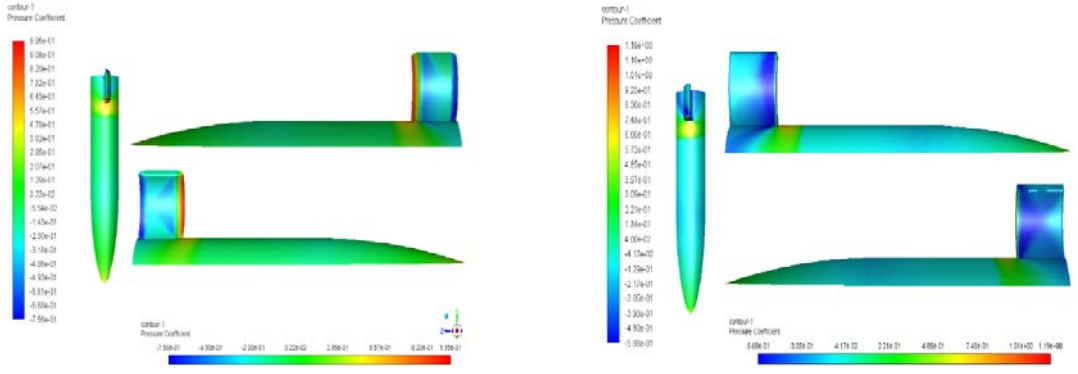

(a) (b)

Figure 11: (a) Sharpened Edged, (b) Blunt edged; Mach 1.2

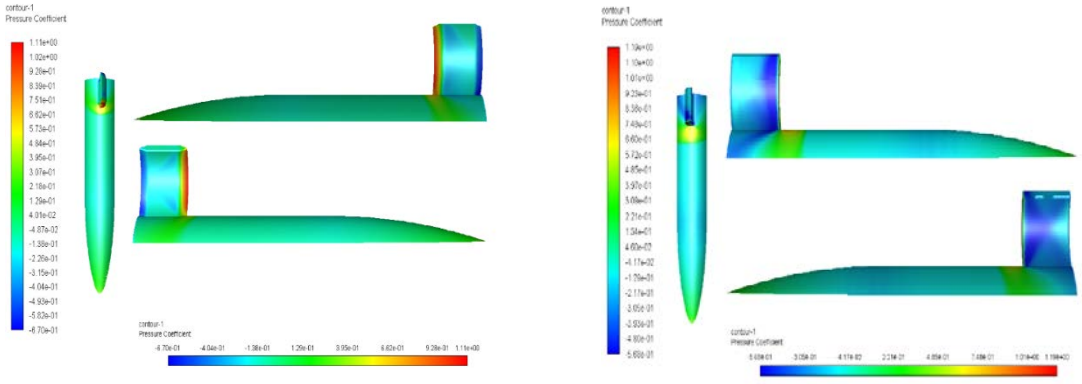

(a) (b)

Figure 12: (a) Sharpened Edged, (b) Blunt edged; Mach 1.4

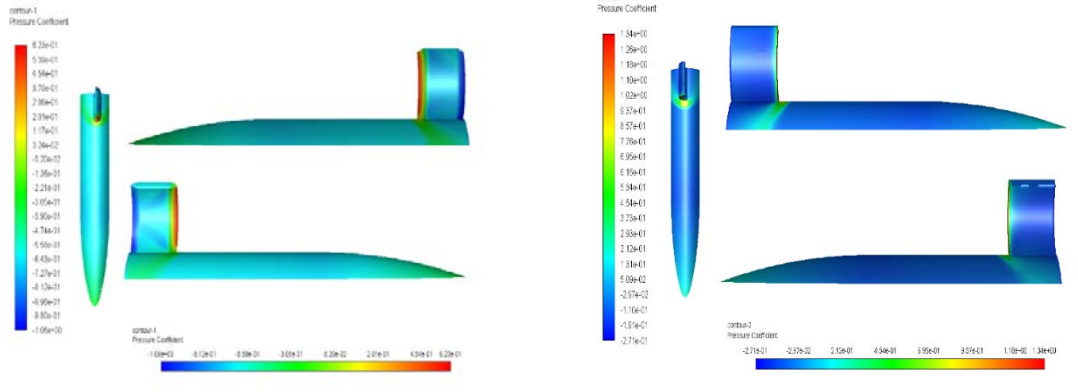

(a) (b)

Figure 13: (a) Sharpened Edged, (b) Blunt edged; Mach 1.6

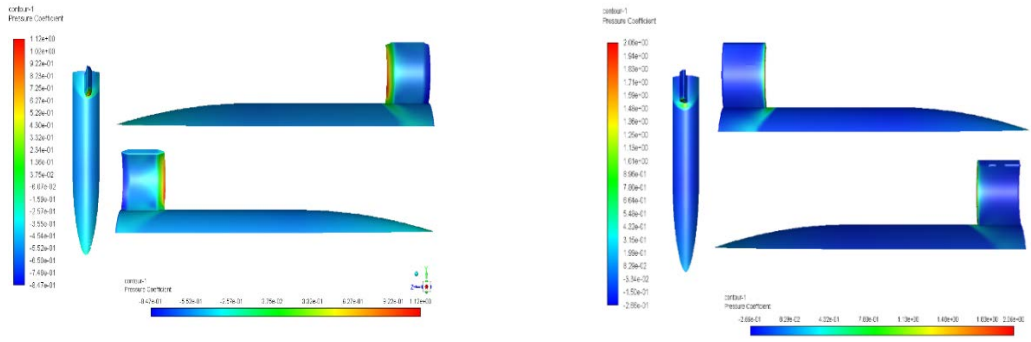

(a) (b)

Figure 14: (a) Sharpened Edged, (b) Blunt edged; Mach 1.8

The second set of images consists of computed pressure coefficient contours along the midplane about sharpened fin missile model at various Mach numbers (Mach 0.8-1.8). Due to the asymmetry of the WAF, a 2-D side view of the flow physics at the midplane is very aptly represented in the following figures *(Figures 15-20)*. The variation in the drag coefficients are better justified on examining the pressure coefficient contours at the midplane. At Mach 0.8 the inception of bow shock formation ahead of the leading edge of the blunt WAF can be seen, this may be the influencing the formation of high-pressure shock region at the nose area of the missile body. This phenomenon is absent in the case of sharpened edged WAF model. Normal shock waves appear at both the types of WAF, thus also ruling out the dis-ambiguity in the compared missile geometries, (excluding the fin) remarkable difference in the pattern of pressure contours can be observed ahead of the leading edges owing to their fin geometries. Oblique shock waves begin to appear at Mach 1.2, in both the sharpened and the blunt edged WAF, however much prominent in the case of the sharpened edged WAF. At Mach 1.2 the oblique shock waves seem to be towards the direction of the concave side of the fin in the case of blunt edged WAF. At Mach 1.4 the oblique shock waves emanating at the nose and the leading edge of the Sharpened WAF are quite prominent. The dissimilarity at the nose of missile in the blunt WAF which was observed at Mach 1.2 are now completely absent at Mach 1.4, which complement the initiation of roll reversal. Following Mach 1.6 the oblique shock waves kick off to align with the flow and become much prominent at Mach 1.8.

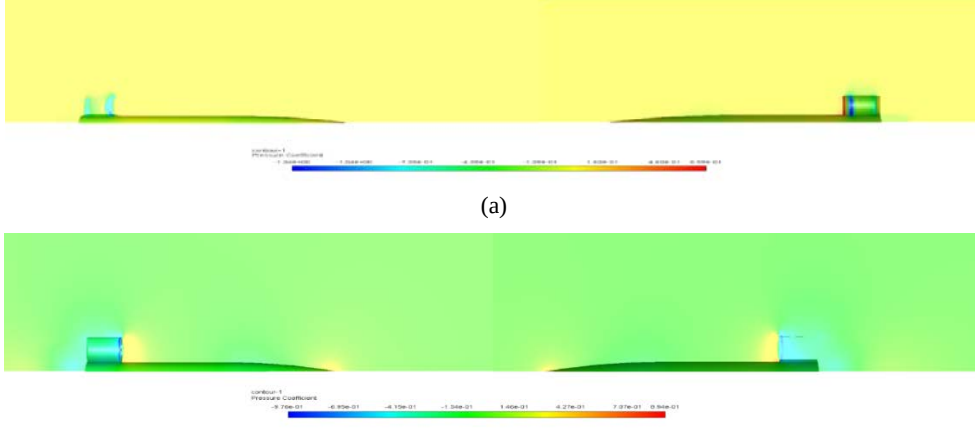

(a)

(b)

Figure 15: (a) Sharpened Edged, (b) Blunt edged; Mach 0.8

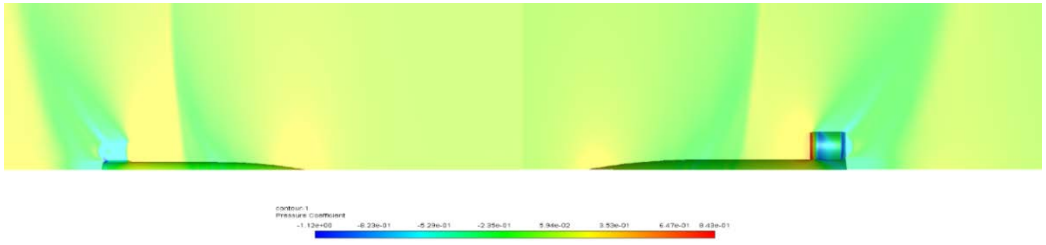

(a)

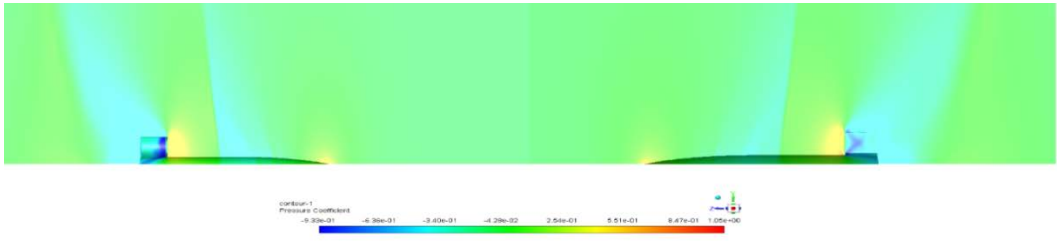

(b)

Figure 16: (a) Sharpened Edged, (b) Blunt edged; Mach 1.0

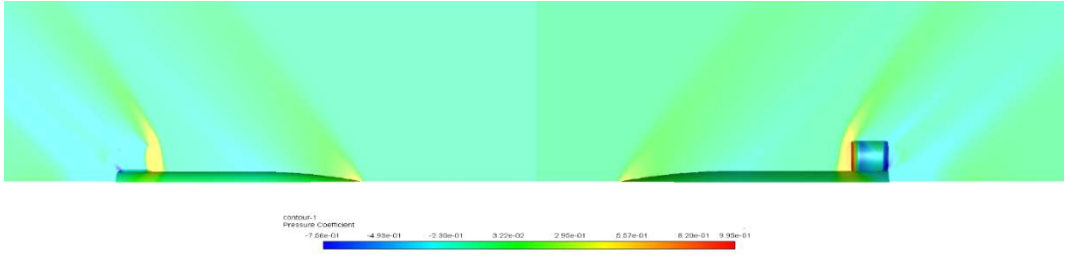

(a)

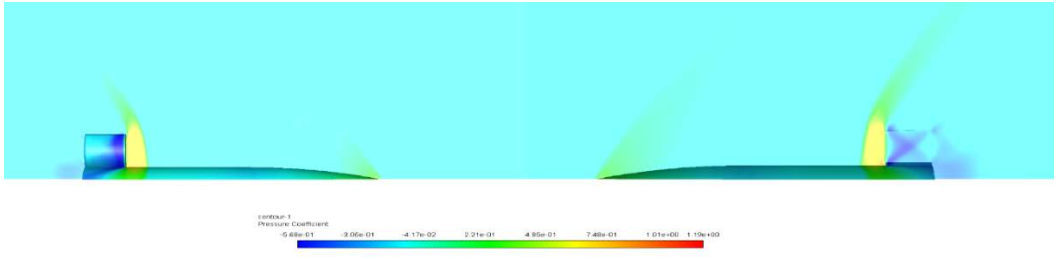

(b)

Figure 17: (a) Sharpened Edged, (b) Blunt edged; Mach 1.2

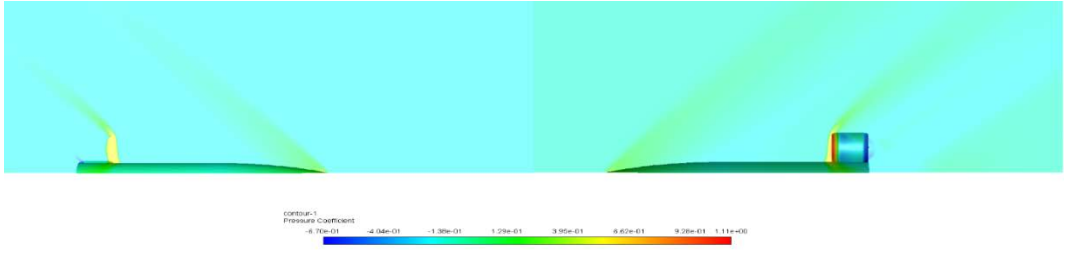

(a)

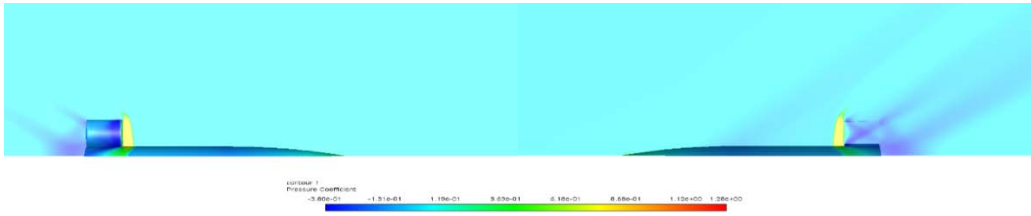

(b)

Figure 18: (a) Sharpened Edged, (b) Blunt edged; Mach 1.4

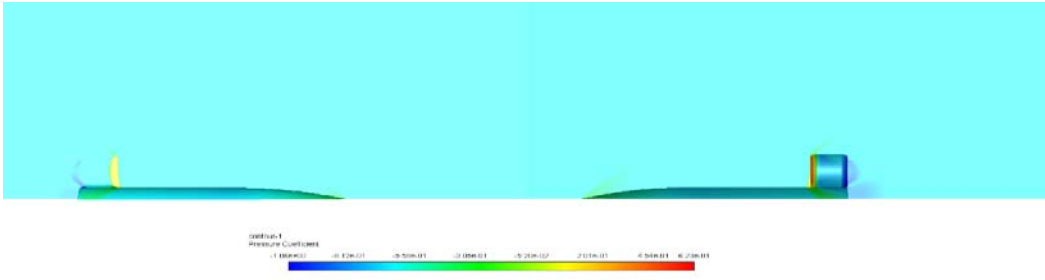

(a)

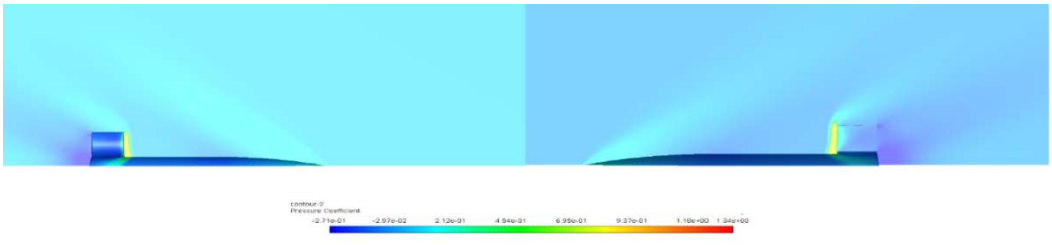

(b)

Figure 19: (a) Sharpened Edged, (b) Blunt edged; Mach 1.6

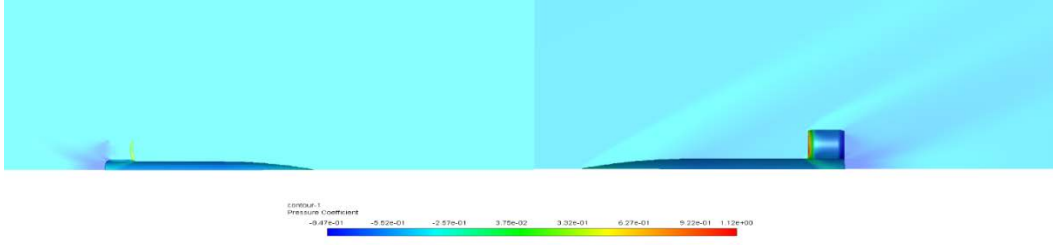

(a)

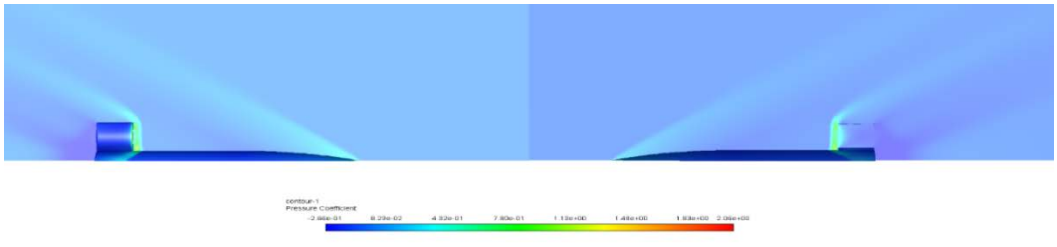

(b)

Figure 20: (a) Sharpened Edged, (b) Blunt edged; Mach 1.8

The third set of images consists of Computed Pressure Coefficient Contours around the Sharpened Fin in the Chordwise Upward Direction starting from the root of the fin (left) to the top tip of the fin (right) *(Figures 21-26)*. Five different positions were selected along the chord planes of the fin starting from the root of the fin till top edge of the fin. Major flow phenomenon occurs at the plane which coincides with the root of the fin. Bow shock formation is quite prominent in the case of blunt edged WAF. Another interesting phenomenon that can be observed is that sharpening of the leading or the trailing edge lessen the influence of the trailing edge on the fluid flow, especially moving in the upward (top) direction. Multiple shock patterns emerge on the WAF with blunt edges, starting at Mach 1.2 till Mach 1.6. The bow shock phenomena remain an attribute of a blunt edged WAF throughout the supersonic regime.

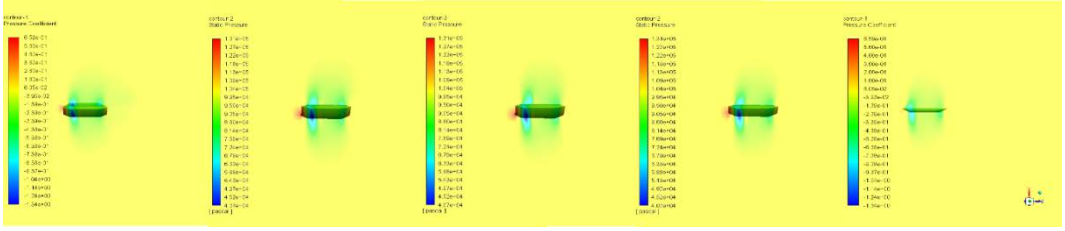

(a)

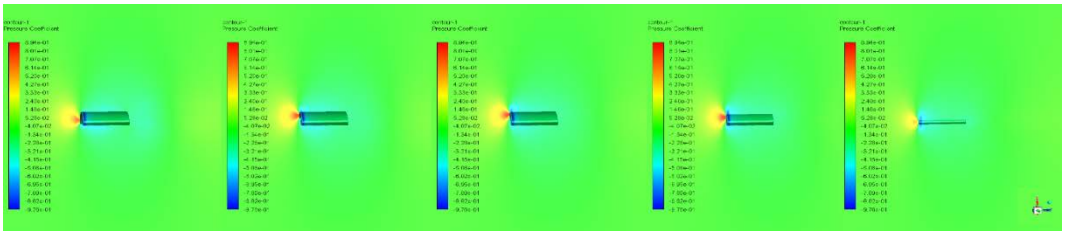

(b)

Figure 21: (a) Sharpened Edged, (b) Blunt edged; Mach 0.8

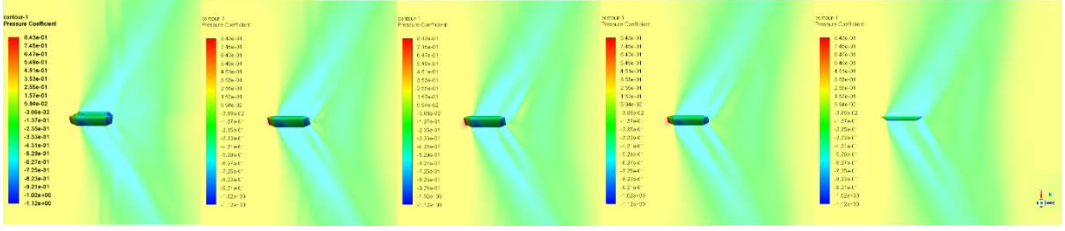

(a)

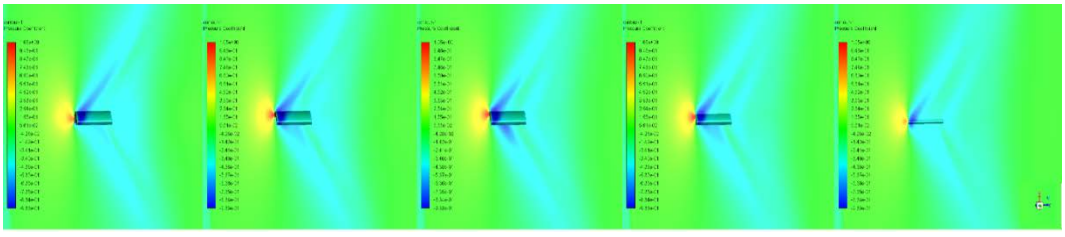

(b)

Figure 22: (a) Sharpened Edged, (b) Blunt edged; Mach 1.0

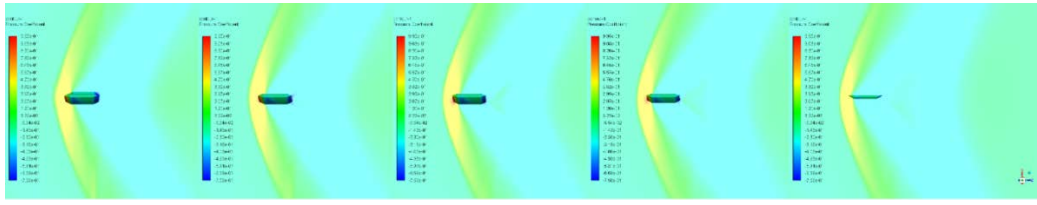

(a)

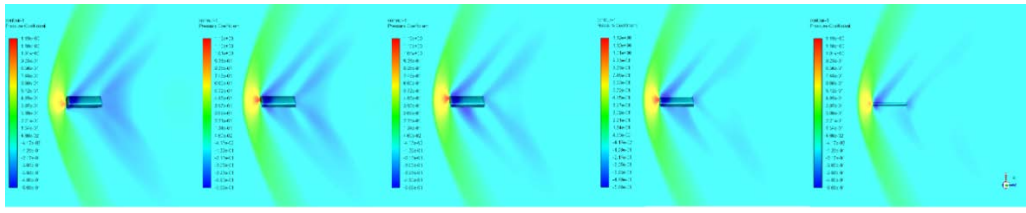

(b)

Figure 23: (a) Sharpened Edged, (b) Blunt edged; Mach 1.2

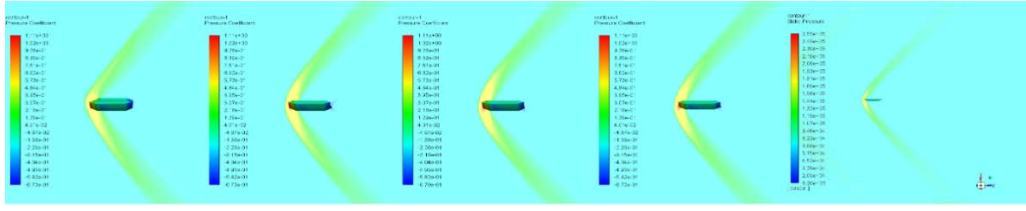

(a)

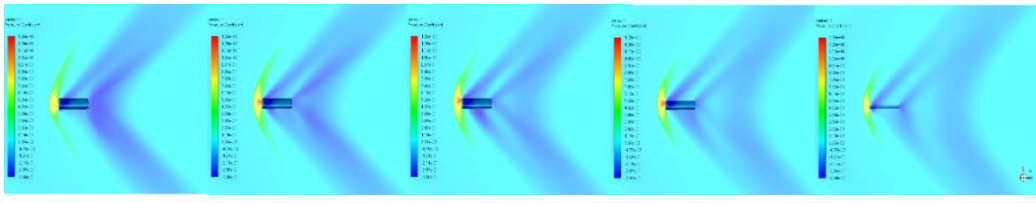

(b)

Figure 24: (a) Sharpened Edged, (b) Blunt edged; Mach 1.4

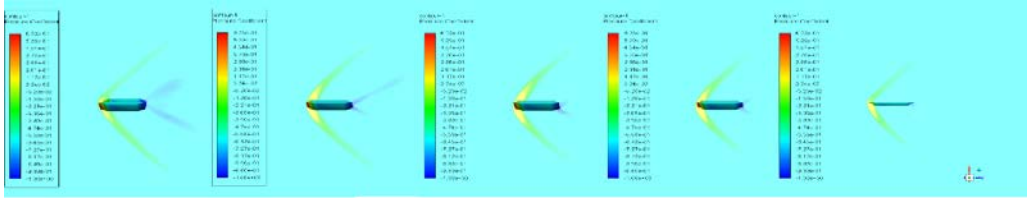

(a)

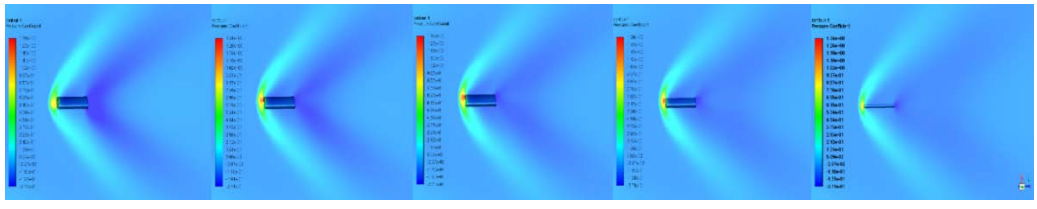

(b)

Figure 25: (a) Sharpened Edged, (b) Blunt edged; Mach 1.6

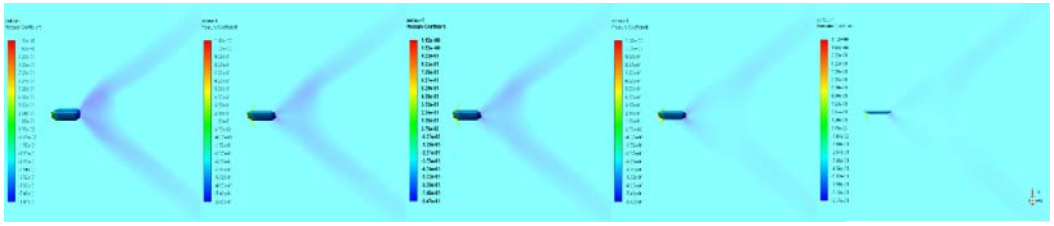

(a)

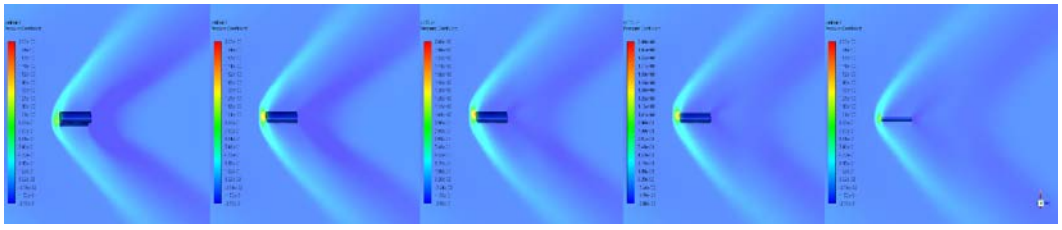

(b)

Figure 26: (a) Sharpened Edged, (b) Blunt edged; Mach 1.8

4. CONCLUSIONS

This paper presented the aerodynamic flow visualisations along with the aerodynamic coefficients for a single WAF mounted on a semi-cylindrical missile body. Two geometries of WAF were considered for better understanding of the flow dynamics in the vicinity of the WAF. These geometries were unique to each other in terms of their leading and trailing edges as well as their alignment with the flow. Choosing a single fin geometry for simulation helped in better meshing around the curved fin and saving the computation time.

The aerodynamics results were computed using realizable two equations κ-ϵ turbulence. The anomalies associated with the WAFs can be attributed to the peculiar-pressure region near the root of the fin. The unequal pressure distributions on both sides of the fins caused the self-induced rolling moment at 0° angle of attack.

The computed aerodynamic coefficients of the single fin model (both Blunt and sharpened edged) were compared with each other, also in addition, using the reference area and reference length, same as that used for a four-fin full missile model, with the previous experimental and computational studies. The computed values showed an agreement with the previous literature. Though these results do not affirm the possibility of computing four-fin performance based on a single-fin computation, it however, can be used for preliminary design of new fin geometries for the studies incorporating reduction of the drag and minimising or eliminating roll reversal. Some of the key findings from the computations are listed below:

- The asymmetry of the fin geometry incubates roll moment, and the shape of the leading and trailing edge influence this rolling moment. The leading edge of the fin majorly influences the flow phenomenon.
- The Drag and Roll moment coefficients of the single WAF model successfully validated, thus may be used as a benchmark for future single WAF computations.
- The pressure concentrations at the leading edge on the fin root (missile juncture) incubated the shock structures. The influence terminates at the leading edge in the case of sharpened edged WAF, however in the case of blunt edged WAF, an influence in the flow pattern is visible throughout the length of the fin.

- The sharpening of edges of the WAF did not completely eliminate the roll reversal phenomenon, however when compared to the Blunt edged WAF, the moment forces in the case of sharpened edged WAFs were smaller.
- The sharpening of the leading and trailing edges of WAF preponed the roll reversal activity. In the case of sharpened edged WAF the roll reversal is reported at Mach ~1.2 whereas in the case of blunt edged WAF the roll reversal is reported at M~1.6.
- There is a motivation to compute different fin geometries using a single fin missile model, at zero-degree angle of attack.

REFERENCES

[1] A. Bagheri, M. Pasandidehfard, and S. A. Tavakoli Sabour, Numerical investigation of aerodynamic effects of opposite wrap-around fins at supersonic speeds, *Proceedings of the Institution of Mechanical Engineers, Part C: Journal of Mechanical Engineering Science*, vol. **0**, no. 0, pp. 1–16, 2018.

[2] A. Seginer and B. Bar-Haim, Aerodynamics of wraparound fins, *J. Spacecr. Rockets*, vol. **20**, no. 4, pp. 339–345, 1983.

[3] A. Seginer and I. Rosenwasser, Magnus effects on spinning transonic finned missiles, *J. Spacecr. Rockets*, vol. **23**, no. 1, pp. 31–38, 1986.

[4] R. E. Vitale and G. L. Abate, Aerodynamic test and analysis of a missile configuration with curved fins, *AIAA J.*, 1992.

[5] E. Air and F. Base, *Roll Motion of a Wraparound Fin Configuration at Subsonic and Transonic Mach Numbers*, no. April, pp. 253–255, 1986.

[6] M. Li, L. K. Abbas, and X. Rui, The Simulation of Wraparound Fins' Aerodynamic Characteristics, *Wseas Transactions on Applied and Theoretical Mechanics*, vol. **10**, pp. 247–252, 2015.

[7] X. Liu, S. J. Tang, and J. Guo, Comparison of the Wrap-Around Fins and the Planar Fins in Aerodynamic Parameter, *Appl. Mech. Mater.*, vol. **444 - 445**, pp. 347–351, 2013.

[8] R. Krishna, R. Surit, A. Kushari, and A. Ghosh, Anomalies in the Flow over Projectile with Wrap-around Fins, *Def. Sci. J.*, vol. **59**, no. 5, pp. 471–484, Sep. 2009.

[9] X. R. Mao, S. X. Yang, and Y. Xu, Coning motion stability of wrap around fin rockets, *Sci. China, Ser. E Technol. Sci.*, vol. **50**, no. 3, pp. 343–350, 2007.

[10] S. Mandic, Analysis of the Rolling Moment Coefficients of a Rockets with Wraparound Fins, *Sci. Rev.*, vol. **LVI**, no. 2, pp. 30–37, 2006.

[11] S.-K. Paek, T.-S. Park, J.-S. Bae, I. Lee, and J. H. Kwon, Computation of Roll Moment for Projectile with Wraparound Fins Using Euler Equation, *J. Spacecr. Rockets*, vol. **36**, no. 1, pp. 53–58, 1999.

[12] H. L. Edge, Computation of the roll moment for a projectile with warp-around fins, *J. Spacecr. Rockets*, vol. **31**, no. 4, pp. 615–620, Jul. 1994.

[13] C. W. Dahike, *The Aerodynamic Characteristics of Wrap-around Fins at Mach Numbers of 0.3 to 3.0*, Redstone Arsenal, Alabama, 1976.

[14] T. C. McIntyre, R. D. W. Bowersox, and L. P. Goss, Effects of Mach number on supersonic wraparound fin aerodynamics, *J. Spacecr. Rockets*, vol. **35**, no. 6, pp. 742–748, 1998.

[15] M. W. Swenson, G. L. Abate, and R. H. Whyte, Aerodynamic Test and Analysis of Wrap-Around Fins at Supersonic Mach Numbers Utilizing Design of Experiments, in *28th Aerospace Sciences Meeting & Exhibit*, 1994.

[16] G. Abate, W. Hathaway, S. Burlington, and A. T. Assoc, Aerodynamic Test and Analysis of Wrap Around Fins with Base Cavities, *AIAA J.*, no. 32nd Aerospace Sciences Meeting 8t Exhibit, 1994.

[17] G. L. Abate and G. L. Winchenbach, Aerodynamics of Missiles with Slotted Fin Configurations, *AIAA J.*, p. 676, 1991.

[18] R. H. Whyter and W. H. Hathaway, Subsonic and Transonic Aerodynamics of a Wraparound Fin Configuration, vol. **9**, no. 6, pp. 627–632, 1986.

[19] R. H. Fournier, *Supersonic aerodynamic characteristics of a series of wrap-around-fin missile configurations*, NASA TM X - 3641, 1977.

[20] J. R. Huffman, C. P. Tilmann, T. A. Buter, and R. D. W. Bowersox, *Experimental Investigation of the Flow Structure in the Vicinity of a Single Wrap-Around Fin at Mach 2.9*, 1996.

[21] C. P. Tilmann, J. R. Huffman, T. A. Buter, R. D. W. Bowersox, Experimental Investigation of the Flow Structure Near a Single Wraparound Fin, vol. **34**, no. 6, 1997.

[22] C. P. Tilmann, J. R. Huffman, T. A. Buter, and R. D. W. Bowersox, Characterization of the flow structure in

the vicinity of a wrap-around fin at supersonic speeds, *Instrumentation*, no. January, 1996.
[23] C. P. Tilmann, T. A. Buter, and R. D. W. Bowersox, Characterization of the Flow field near a Wrap-Around Fin at Mach 2.8, *J. Aircr.*, vol. **35**, no. 6, pp. 868–875, 1998.
[24] C. P. Tilmann, *Numerical and Experimental Investigation of the Flowfield Near a Wrap-Around Fin*, 1997.
[25] B. S. Baldwin, H. Lomax, and N. Ames, Thin-layer approximation and algebraic model for separated turbulentflows, *16th Aerosp. Sci. Meet. Huntsville,AL,U.S.A.*
[26] A. L. Gregg and T. Cook, Analysis of missile configurations with wrap-around fins using computational fluid dynamics, *Flight Simul. Technol.*, 1993.
[27] N. Sharma and R. Kumar, A Ready Reckoner of CFD for Wrap-around Fins, *INCAS Bull.*, vol. **11**, no. 2, pp. 155–170, Jun. 2019.
[28] N. Sharma and R. Kumar, The simulation of single wraparound fin on a semi-cylindrical missile body, *Aircr. Eng. Aerosp. Technol.*, vol. **92**, no. 3, pp. 418–427, Jan. 2020.
[29] N. Sharma and R. Kumar, Investigation of flow‐field around a single generic planar fin using CFD, *SN Appl. Sci.*, vol. **2**:63, no. January 2020, p. 12, 2020.
[30] N. Sharma, P. Saini, H. Chaudhary, G. Nagi, and R. Kumar, Comparison of Flow field in the proximity of A Single Planar & Wrap-around Fin, *Int. J. Aviat. Aeronaut. Aerosp.*, vol. **6**, no. 4, p. 31, 2019.
[31] N. Sharma and R. Kumar, Missile Grid Fins Analysis using Computational Fluid Dynamics: A Systematic Review, *Incas Bull.*, vol. **11**, no. 1, pp. 151–169, 2019.
[32] Liu, Computational Fluid Dynamics A Practical Approach, *Igarss 2014*, 2014.
[33] * * * ANSYS, Chapter 24. Using the Solver, pp. 1–114, 2001.